

Exact Large Deviation Functional of a Stationary Open Driven Diffusive System: The Asymmetric Exclusion Process

B. Derrida,^{1,3} J. L. Lebowitz,^{2,3,4} and E. R. Speer²

Received May 1, 2002; accepted September 9, 2002

We consider the asymmetric exclusion process (ASEP) in one dimension on sites $i = 1, \dots, N$, in contact at sites $i = 1$ and $i = N$ with infinite particle reservoirs at densities ρ_a and ρ_b . As ρ_a and ρ_b are varied, the typical macroscopic steady state density profile $\bar{\rho}(x)$, $x \in [a, b]$, obtained in the limit $N = L(b-a) \rightarrow \infty$, exhibits shocks and phase transitions. Here we derive an exact asymptotic expression for the probability of observing an arbitrary macroscopic profile $\rho(x)$: $P_N(\{\rho(x)\}) \sim \exp[-L\mathcal{F}_{[a,b]}(\{\rho(x)\}; \rho_a, \rho_b)]$, so that \mathcal{F} is the large deviation functional, a quantity similar to the free energy of equilibrium systems. We find, as in the symmetric, purely diffusive case $q = 1$ (treated in an earlier work), that \mathcal{F} is in general a non-local functional of $\rho(x)$. Unlike the symmetric case, however, the asymmetric case exhibits ranges of the parameters for which $\mathcal{F}(\{\rho(x)\})$ is not convex and others for which $\mathcal{F}(\{\rho(x)\})$ has discontinuities in its second derivatives at $\rho(x) = \bar{\rho}(x)$. In the latter ranges the fluctuations of order $1/\sqrt{N}$ in the density profile near $\bar{\rho}(x)$ are then non-Gaussian and cannot be calculated from the large deviation function.

KEY WORDS: Large deviations; asymmetric simple exclusion process; open system; stationary nonequilibrium state.

1. INTRODUCTION

Stationary nonequilibrium states (SNS) maintained by contact with infinite thermal reservoirs at the system boundaries are objects of great theoretical

Dedicated to Michael E. Fisher on the occasion of his seventieth birthday.

¹ Laboratoire de Physique Statistique, École Normale Supérieure, 24 rue Lhomond, 75005 Paris, France; e-mail: derrida@lps.ens.fr.

² Department of Mathematics, Rutgers University, New Brunswick, New Jersey 08903; e-mail: lebowitz@math.rutgers.edu, speer@math.rutgers.edu.

³ Also School of Mathematics, Institute for Advanced Study, Princeton, New Jersey 08540.

⁴ Also Department of Physics, Rutgers.

and practical interest.⁽¹⁻⁹⁾ One is tempted to think that, at least when the gradients and fluxes induced by the reservoirs are small, the full system behavior is just that of a union of subsystems, each in local equilibrium, with spatially varying particle and energy densities or equivalently local chemical potential and temperature. This is, however, not the entire story, as is clear when one considers the paradigm of such systems, a fluid in contact with a thermal reservoir at temperature T_a at the top and one at temperature T_b at the bottom, the Rayleigh–Bénard system.⁽⁶⁾ In this system there are long range correlations not present in equilibrium systems, which have been measured by neutron scattering experiments. This system exhibits, when $T_b - T_a$ exceeds some positive critical value, dynamic phase transitions corresponding to the formation of different patterns of heat and mass flow as the parameters are varied. These are due to macroscopic instabilities, caused by gravity, but are not derivable at present, despite various attempts,⁽⁹⁾ in terms of a microscopic theory of SNS such as that provided by statistical mechanics in the case $T_a = T_b$, when the system is an equilibrium one.

In this paper we study the SNS of a model system which, despite its simplicity, has some phase transitions and exhibits many phenomena, such as long range correlations and non-Gaussian fluctuations, which are very different from those of systems in local thermal equilibrium. For this system the weights of the microscopic configurations are known and the typical behavior has been deduced from them.⁽¹²⁾ Here we determine—again from the microscopic weights—the probabilities of various atypical macroscopic behaviors, that is, of large deviations.

The model we consider is the SNS of the open asymmetric simple exclusion process (ASEP):^(10,11) a lattice gas on a chain of N sites which we index by i , $1 \leq i \leq N$. At any given time t , each site is either occupied by a single particle or is empty, and the system evolves according to the following dynamics. In the interior of the system ($2 \leq i \leq N-1$), a particle attempts to jump to its right neighboring site with rate 1 and to its left neighboring site with rate q (with $0 \leq q < 1$). The jump is completed if the target site is empty, otherwise nothing happens. The boundary sites $i = 1$ and $i = N$ are connected to particle reservoirs and their dynamics is modified as follows: if site 1 is empty, it becomes occupied at rate α by a particle from the left reservoir; if it is occupied, the particle attempts to jump to site 2 (succeeding if this site is empty) with rate 1. Similarly, if site N is occupied, the particle may either jump out of the system (into the right reservoir) at rate β or to site $N-1$ at rate q .

More generally, one can also consider the ASEP with the above dynamical rules supplemented by an output rate γ at $i = 1$ and an input rate δ at $i = N$. However, the calculations in the case of nonzero γ or δ are

more complicated, and for that reason we limit our analysis in the present paper to the case $\gamma = \delta = 0$.

It is convenient to introduce the two parameters

$$\rho_a = \frac{\alpha}{1-q}, \quad \rho_b = 1 - \frac{\beta}{1-q}; \quad (1.1)$$

we require that $0 \leq \alpha, \beta \leq 1-q$, so that $0 \leq \rho_a, \rho_b \leq 1$. These parameters have a natural interpretation as reservoir densities. In particular, when $\rho_a = \rho_b$ the steady state of the system is a Bernoulli measure at constant density ρ_a , that is, each site is occupied independently with probability ρ_a ; this may be seen for example from the so-called "matrix method" (see Section 4). In general, then, we interpret ρ_a and ρ_b as the densities of particles in the left and right reservoirs, respectively.

In what follows we are interested by the large N limit and we will describe the system in terms of a macroscopic variable x ; for later discussions it is convenient to allow x to belong to an arbitrary interval $[a, b]$. Thus the microscopic and macroscopic coordinates are related by $x = a + (b-a) i/N$, the ratio L between the macroscopic and the microscopic lengths is $L = N/(b-a)$, and there are $N = L(b-a)$ sites on the macroscopic interval $[a, b]$.

The goal of the present work is to calculate the large N behavior of $P_N(\{\rho(x)\})$, the probability of seeing a macroscopic profile $\rho(x)$ for $a < x < b$ in the steady state for a system of $N = L(b-a)$ sites. This probability $P_N(\{\rho(x)\})$ can be thought of as the sum of the probabilities of all microscopic configurations such that in each box of $L dx$ sites (with $dx \ll 1$ and $L dx \gg 1$), the number of particles is close to $L\rho(x) dx$. The ratio $\log(P_N(\{\rho(x)\}))/L$ has a well defined limit for large L ,

$$\lim_{L \rightarrow \infty} \frac{\log P_N(\{\rho(x)\})}{L} \equiv -\mathcal{F}_{[a,b]}(\{\rho(x)\}; \rho_a, \rho_b), \quad (1.2)$$

which depends on $b-a$, on the density profile $\rho(x)$, and on the reservoir densities. \mathcal{F} is called the large deviation functional (LDF) of the system.

When $\rho_a = \rho_b$, the steady state is a Bernoulli measure, as described above. This measure is just the equilibrium state of a system of particles, noninteracting except for the hard-core exclusion, at chemical potential $\log(\rho_a/(1-\rho_a))$. For this system the LDF can be computed by elementary means, and is given by⁽¹³⁻¹⁵⁾

$$\mathcal{F}_{[a,b]}(\{\rho(x)\}; \rho_a, \rho_a) = \int_a^b \left[\rho(x) \log \frac{\rho(x)}{\rho_a} + (1-\rho(x)) \log \frac{1-\rho(x)}{1-\rho_a} \right] dx. \quad (1.3)$$

The present paper is devoted primarily to the derivation of the exact expression of \mathcal{F} in the case $\rho_a \neq \rho_b$.

1.1. Additivity and Large Deviations in the ASEP

In our earlier work^(16,15) on the large deviation functional for the symmetric simple exclusion process, corresponding to equal jump rates to the left and right, i.e., to $q = 1$, we were able to use the matrix method^(12, 17–19) to calculate directly the probability of a given macroscopic profile $\rho(x)$ by summing the probabilities of all configurations corresponding to that profile. For the asymmetric model, however, such a direct calculation is *a priori* more complicated. For that reason, we follow here a different path, which has its origin in an *a posteriori* observation made in ref. 15. We noted there that while the large deviation functional for the symmetric case is nonlocal, it possesses a certain “additivity” property. For the ASEP we first derive an additivity property, similar to that of the symmetric model, and from that obtain \mathcal{F} . The derivations are given in Section 5.

The addition formula involves a function \mathcal{H} related to \mathcal{F} by

$$\mathcal{H}_{[a,b]}(\{\rho(x)\}; \rho_a, \rho_b) = \mathcal{F}_{[a,b]}(\{\rho(x)\}; \rho_a, \rho_b) + (b-a) K(\rho_a, \rho_b), \quad (1.4)$$

where $K(\rho_a, \rho_b)$ does not depend on $\rho(x)$. Since the dynamics in the bulk is driven from left to right (for $0 \leq q < 1$), the roles played by the left and the right reservoirs (1.1) are not symmetric and the additivity relation and the expressions for $K(\rho_a, \rho_b)$ in (1.4) and for $\mathcal{F}_{[a,b]}(\{\rho(x)\}; \rho_a, \rho_b)$ depend on whether $\rho_a > \rho_b$ or $\rho_a < \rho_b$.

1.1.1. The Case $\rho_a \geq \rho_b$

When $\rho_a \geq \rho_b$ the constant in (1.4) is

$$K(\rho_a, \rho_b) = \sup_{\rho_b \leq \rho \leq \rho_a} \log[\rho(1-\rho)], \quad (1.5)$$

and the additivity relation, obtained in Section 5 below, is that for any c with $a < c < b$,

$$\begin{aligned} & \mathcal{H}_{[a,b]}(\{\rho(x)\}; \rho_a, \rho_b) \\ &= \sup_{\rho_b \leq \rho_c \leq \rho_a} [\mathcal{H}_{[a,c]}(\{\rho(x)\}; \rho_a, \rho_c) + \mathcal{H}_{[c,b]}(\{\rho(x)\}; \rho_c, \rho_b)]. \end{aligned} \quad (1.6)$$

Equation (1.6) expresses a relation between the large deviation function of the whole system and those of two subsystems connected at the break point to a reservoir at an appropriate density ρ_c .

Once we have the additivity relation (1.6), the derivation of the large deviation functional is simple, and we give it here. We divide our system into n parts of equal length and apply (1.6) n times; this will introduce intermediate reservoir densities $\rho_a \equiv \rho_0 \geq \rho_1 \geq \dots \geq \rho_n \equiv \rho_b$. For very large n , most of the intervals must have reservoir densities ρ_{k-1}, ρ_k at their boundaries which are nearly equal, and the LDF for these intervals is approximately given by (1.3) (with ρ_a there replaced by $\rho_{k-1} \simeq \rho_k$). On the other hand, the total length of the intervals for which this is not true will approach 0 for large n . Now taking the $n \rightarrow \infty$ limit and introducing a function $F(x)$ as the interpolation of the values $\rho_0, \rho_1, \dots, \rho_n$, we are lead directly to a formula for the large deviation functional:

$$\begin{aligned} \mathcal{F}_{[a,b]}(\{\rho(x)\}; \rho_a, \rho_b) &= -(b-a) K(\rho_a, \rho_b) + \sup_{F(x)} \int_a^b dx \rho(x) \log[\rho(x)(1-F(x))] \\ &\quad + (1-\rho(x)) \log[(1-\rho(x)) F(x)], \end{aligned} \tag{1.7}$$

where the supremum is over all *monotone nonincreasing* functions $F(x)$ which for $a \leq x < y \leq b$ satisfy

$$\rho_a = F(a) \geq F(x) \geq F(y) \geq F(b) = \rho_b. \tag{1.8}$$

This supremum is achieved at a certain function $F_\rho(x)$. Note that without the constraints (1.8) one would have $F_\rho(x) = 1 - \rho(x)$. The monotonicity requirement, however, makes the determination of F_ρ more subtle (see Section 3.1) and the expression of \mathcal{F} nonlocal. This will be at the origin of most of its interesting properties.

1.1.2. The Case $\rho_a \leq \rho_b$

When $\rho_a \leq \rho_b$ the constant in (1.4) is

$$K(\rho_a, \rho_b) = \min[\log \rho_a(1-\rho_a), \log \rho_b(1-\rho_b)], \tag{1.9}$$

and the additivity relation, again derived in Section 5, is

$$\begin{aligned} \mathcal{H}_{[a,b]}(\{\rho(x)\}; \rho_a, \rho_b) &= \min_{\rho_c = \rho_a, \rho_b} [\mathcal{H}_{[a,c]}(\{\rho(x)\}; \rho_a, \rho_c) + \mathcal{H}_{[c,b]}(\{\rho(x)\}; \rho_c, \rho_b)]. \end{aligned} \tag{1.10}$$

By an argument similar to that which led to (1.7), we obtain the formula

$$\begin{aligned}
 \mathcal{F}_{[a,b]}(\{\rho(x)\}; \rho_a, \rho_b) &= -(b-a) K(\rho_a, \rho_b) \\
 &+ \inf_{a \leq y \leq b} \left\{ \int_a^y dx \rho(x) \log[\rho(x)(1-\rho_a)] + (1-\rho(x)) \log[(1-\rho(x)) \rho_a] \right. \\
 &\left. + \int_y^b dx \rho(x) \log[\rho(x)(1-\rho_b)] + (1-\rho(x)) \log[(1-\rho(x)) \rho_b] \right\}.
 \end{aligned} \tag{1.11}$$

The fact that for each $\rho(x)$ one has to find in (1.11) the infimum over y makes, in this case too, the large deviation function nonlocal.

It is interesting to note that the formulas (1.7) and (1.11) for the large deviation function do not depend on q .

1.2. Outline of the Paper

In Section 2 we review briefly some known results on the open ASEP, emphasizing the phase diagram. In Section 3 we give a summary of our results which follow as consequences of the formulas (1.7) and (1.11) for the large deviation function. In Section 4 we recall the matrix method for carrying out exact calculations in the ASEP and give several results obtained by this method which are relevant to our considerations here. Then in Section 5 we give the derivation of the addition formulas (1.6) and (1.10). An unexpected consequence of our results, discussed in Section 6, is that the correlations in the steady state are not related in any simple manner to the large deviation function. We also show in that section that the fluctuations of the number of particles in any box of size Lx , with $0 < x < 1$, are not Gaussian for certain ranges of the parameters ρ_a, ρ_b . Section 7 gives some concluding remarks, and certain more technical questions are discussed in appendices.

2. THE STEADY STATE OF THE ASEP WITH OPEN BOUNDARY CONDITIONS

We describe here the phase diagram of the ASEP with open boundary conditions, which has been obtained by various methods.^(12, 18-21) As indicated above, we consider here only the case $\gamma = \delta = 0$, $0 \leq \alpha, \beta \leq 1 - q$.

The phase diagram is given in Fig. 1, where we have chosen as parameters the densities ρ_a and ρ_b (1.1) of the two reservoirs. There are three phases: a low density phase A with a constant density $\bar{\rho}(x) = \rho_a$ in the

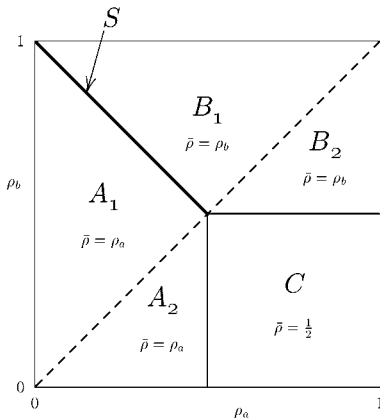


Fig. 1. The phase diagram of the open ASEP.

bulk, a high density phase B with a density $\bar{\rho}(x) = \rho_b$, and a maximal current phase C with a density $\bar{\rho}(x) = 1/2$. The current in each phase is given by $J = (1 - q) \bar{\rho}(1 - \bar{\rho})$. The transition lines between these phases are second order phase transitions where $\bar{\rho}(x)$ is a continuous function of ρ_a and ρ_b , except for the boundary S ($\rho_a = 1 - \rho_b < 1/2$) between phase A and B , where the transition is first order: $\bar{\rho}(x)$ jumps from ρ_a to ρ_b . On the line S the typical configurations are shocks between phase A with density ρ_a at the left of the shock and phase B with density ρ_b at the right of the shock:

$$\rho_y(x) \equiv \rho_a \Theta(y - x) + \rho_b \Theta(x - y), \tag{2.1}$$

with Θ the Heaviside function. The position y of the shock is uniformly distributed along the system,^(22, 23) and as a result the average profile is linear: $\langle \bar{\rho}(x) \rangle = \rho_a(1 - x) + \rho_b x$.

This phase diagram can be understood easily in heuristic terms. First consider an infinite one dimensional lattice on which the initial configuration is a Bernoulli distribution at density ρ_a to the left of the origin and ρ_b to the right of the origin. If $\rho_a < \rho_b$, this initial condition produces a shock moving at velocity $(1 - \rho_a - \rho_b)(1 - q)$; thus in the long time limit, the distribution near the origin is Bernoulli, with density ρ_a if $\rho_a + \rho_b < 1$ and density ρ_b if $\rho_a + \rho_b > 1$. On the other hand if $\rho_a > \rho_b$, the profile becomes a rarefaction fan: $\rho(x, t) = \rho_a$ if $x \leq x_a(t)$, $\rho(x, t) = \rho_a + (\rho_b - \rho_a)(x - x_a(t)) / (x_b(t) - x_a(t))$ if $x_a(t) < x < x_b(t)$, and $\rho(x, t) = \rho_b$ if $x_b(t) \leq x$, with $x_\alpha(t) = (1 - q)(1 - 2\rho_\alpha) t$, $\alpha = a, b$. If $1/2 < \rho_b < \rho_a$ then the entire fan moves away to the left, if $\rho_b < \rho_a < 1/2$ then it moves away to the right, and if $\rho_b < 1/2 < \rho_a$ then the origin remains in the fan for all time. These three cases give rise in the long time limit to Bernoulli distributions at the

origin, with densities ρ_a , ρ_b , and $1/2$, respectively (see, e.g., ref. 24 and references therein).

If now we consider the finite system with left and right reservoirs at densities ρ_a and ρ_b , and start with a Bernoulli distribution at density ρ_a at the left of some point in the bulk far from the boundaries, and ρ_b at the right of this point, then the evolution will be the same as in the infinite system until the shock or the fan reaches the boundary, leading, for the asymptotic density in the bulk, to what is given in the phase diagram. This idea is at the basis of what has been done recently by Popkov and Schütz^(25, 26) to predict boundary induced phase diagrams in more general cases.

The dashed line $\rho_a = \rho_b$ ($\alpha + \beta = 1 - q$) in Fig. 1 separates what we will call the *shock region* $\rho_a < \rho_b$ and the *fan region* $\rho_a > \rho_b$. On this line the measure reduces to a Bernoulli measure at density ρ_a (see Section 4) and the large deviation function is given by (1.3). The line plays no role in the phase diagram for the typical profile $\bar{\rho}$ but separates phases *A* and *B* into two subphases, A_1, A_2 and B_1, B_2 , which, as we have seen in Section 1, can be distinguished by the different expressions (1.7), (1.11) for the large deviation function in these regions.

3. CONSEQUENCES OF THE LARGE DEVIATION FORMULA FOR THE ASEP

In this section we describe some consequences of formulas (1.7) and (1.11) for the large deviation function. It is convenient to write (1.5) and (1.9) in the unified form

$$K(\rho_a, \rho_b) = \log \bar{\rho}(1 - \bar{\rho}), \quad (3.1)$$

where $\bar{\rho} = \bar{\rho}(x)$ depends on ρ_a and ρ_b and is obtained from the phase diagram, Fig. 1. Note that $\bar{\rho}$, the bulk density on the macroscopic scale (on which boundary profiles are invisible) is independent of x , except on the line S ; there $\bar{\rho}$ can be any shock profile $\rho_y(x)$ (2.1), but the value of $K(\rho_a, \rho_b)$ is independent of the shock position y since $\rho_a + \rho_b = 1$ on S . We also introduce the notation

$$h(r, f; \bar{\rho}) = r \log \frac{r}{f} + (1 - r) \log \frac{1 - r}{1 - f} + \log \frac{f(1 - f)}{\bar{\rho}(1 - \bar{\rho})}, \quad (3.2)$$

so that (1.7) and (1.11) become respectively

$$\begin{aligned} & \mathcal{F}_{[a, b]}(\{\rho(x)\}; \rho_a, \rho_b) \\ &= \sup_{F(x)} \int_a^b dx h(\rho(x), F(x); \bar{\rho}) = \int_a^b dx h(\rho(x), F_\rho(x); \bar{\rho}), \end{aligned} \quad (3.3)$$

for $\rho_a > \rho_b$, and

$$\begin{aligned} & \mathcal{F}_{[a,b]}(\{\rho(x)\}; \rho_a, \rho_b) \\ &= \inf_{a \leq y \leq b} \left\{ \int_a^y dx h(\rho(x), \rho_a; \bar{\rho}) + \int_y^b dx h(\rho(x), \rho_b; \bar{\rho}) \right\}, \end{aligned} \quad (3.4)$$

for $\rho_a < \rho_b$, where again $\bar{\rho}$ is determined from ρ_a, ρ_b through the phase diagram. Note that $h(r, f; \bar{\rho})$ is strictly convex in r for fixed $f, \bar{\rho}$, with a minimum at $r = f$.

3.1. Construction of the Function F_ρ

There is a rather simple way of constructing the optimizing function $F_\rho(x)$ in (3.3). If $g(x)$ is any function defined on the interval $[a, b]$, its concave envelope g^* is the smallest concave function that $g^*(x) \geq g(x)$ on $[a, b]$. Now let $G_\rho(x)$ be defined for $a \leq x \leq b$ by

$$G_\rho(x) = \text{Concave Envelope} \left\{ \int_a^x (1 - \rho(y)) dy \right\}; \quad (3.5)$$

then F_ρ is obtained by cutting off $G'_\rho(x)$ at ρ_a and ρ_b :

$$F_\rho(x) = \begin{cases} \rho_a, & \text{if } G'(x) \geq \rho_a. \\ G'(x), & \text{if } \rho_b \leq G'(x) \leq \rho_a, \\ \rho_b, & \text{if } G'(x) \leq \rho_b, \end{cases} \quad (3.6)$$

This construction is verified in Appendix A.

In Fig. 2 we illustrate the construction for the density profile $\rho(x) = 0.5 - 0.45 \cos 3\pi x$, with $\rho_a = 0.8$ and $\rho_b = 0.0$.

As a second example, suppose that $\rho(x)$ is a constant profile: $\rho(x) = r$. Then the expression in brackets in (3.5) is concave and hence equal to $G_\rho(x)$, so that $G'_\rho(x) = 1 - r$ and F_ρ is constant: $F_\rho = \rho_a$ if $r < 1 - \rho_a$, $F_\rho = 1 - r$ if $1 - \rho_a \leq r \leq 1 - \rho_b$, and $F_\rho = \rho_b$ if $1 - \rho_b < r$. In particular, taking $r = \bar{\rho}$ we find that

$$F_{\bar{\rho}} = \bar{\rho}. \quad (3.7)$$

For (i) in region A_2 , where $1/2 > \rho_a > \rho_b$, $r = \rho_a < 1 - \rho_a$ and so $F_\rho = \rho_a = \bar{\rho}$; (ii) in region C , where $\rho_a > 1/2 > \rho_b$, $r = 1/2$ and so $F_\rho = 1 - r = 1/2 = \bar{\rho}$; (iii) in region B_2 , where $\rho_a > \rho_b > 1/2$, $r = \rho_b > 1 - \rho_b$ and so $F_\rho = \rho_b = \bar{\rho}$.

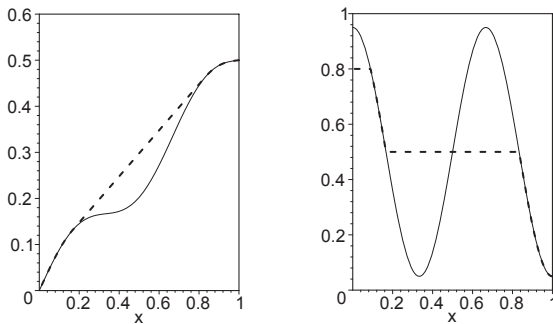


Fig. 2. The concave envelope construction for $\rho_a = 0.8$, $\rho_b = 0.0$, and $\rho(x) = 0.5 - 0.45 \cos 3\pi x$. On the left we show $\int_0^x (1 - \rho(y)) dy$ (solid line) and its concave envelope $G_\rho(x)$ (dashed line); on the right $1 - \rho(x)$ (solid) and $F_\rho(x)$ (dashed).

3.2. The Most Likely Profile

We will show in this section that the most likely profile is always given by $\rho(x) = \bar{\rho}$, with $\bar{\rho}$ given by Fig. 1; specifically, that $\mathcal{F}_{[a,b]}(\{\rho(x)\}; \rho_a, \rho_b) \geq 0$ for all $\rho(x)$, that $\mathcal{F}_{[a,b]}(\{\bar{\rho}\}; \rho_a, \rho_b) = 0$, and that $\mathcal{F}_{[a,b]}(\{\rho(x)\}; \rho_a, \rho_b) > 0$ if $\rho(x) \neq \bar{\rho}$. This is of course expected and in fact represents an alternate way to obtain the phase diagram of Fig. 1.

To obtain the most likely profile in the fan region $\rho_a \geq \rho_b$, we note that (3.3), (3.7), and the convexity of $h(r, f; \bar{\rho})$ in r imply that

$$\begin{aligned} \mathcal{F}_{[a,b]}(\{\rho(x)\}; \rho_a, \rho_b) &= \int_a^b dx h(\rho(x), F_\rho(x); \bar{\rho}) \\ &\geq \int_a^b dx h(\rho(x), F_{\bar{\rho}}; \bar{\rho}) \\ &\geq \int_a^b dx h(F_{\bar{\rho}}, F_{\bar{\rho}}; \bar{\rho}) = 0. \end{aligned} \tag{3.8}$$

Moreover, if $\rho(x) = \bar{\rho}$ then equality holds throughout (3.8), so that the minimum value of \mathcal{F} is zero and $\bar{\rho}$ is a minimizer; otherwise the second inequality is strict, from which it follows that this minimizer is unique.

In the shock region $\rho_a < \rho_b$, we observe that for fixed y , $a \leq y \leq b$, the right side of (3.4) is minimized by the unique choice $\rho(x) = \rho_a$ for $a \leq x < y$, $\rho(x) = \rho_b$ for $y < x \leq b$. Minimizing over y then implies that, except on the first order line S , the optimal profile is again constant with value $\bar{\rho}$, and is unique; again the corresponding minimum value of \mathcal{F} is zero. On S all values of y give the value zero for \mathcal{F} , so that the shock profiles $\rho_y(x)$ of (2.1) form a one parameter family of minimizing profiles.

Note that a knowledge of the large deviation functional is not sufficient to determine the distribution of the shock position y mentioned in Section 2.

3.3. Convexity

In the fan region $\rho_a \geq \rho_b$, the LDF $\mathcal{F}_{[a,b]}(\{\rho(x)\}; \rho_a, \rho_b)$ is a strictly convex functional of $\rho(x)$, since by (3.3) it is the maximum (over the functions $F(x)$) of strictly convex functionals of $\rho(x)$. This is also true in the symmetric case^(16, 15) and in equilibrium systems not at a phase transition. In the shock region $\rho_a < \rho_b$, on the contrary, \mathcal{F} is not convex. This is most easily verified on the line S , since it follows from Section 3.2 that on S a superposition of minimizing profiles (2.1), $\rho(x) = \lambda \rho_y(x) + (1 - \lambda) \rho_z(x)$, $y \neq z$, satisfies $\mathcal{F}(\{\rho(x)\}) > 0$ for $0 < \lambda < 1$. But we will also see in Section 3.5 below that for every ρ_a, ρ_b there is a constant profile $\rho(x) = r^*$ near which \mathcal{F} is not convex.

3.4. Suppression and Enhancement of Large Deviations

The LDF in the fan region $\rho_a > \rho_b$ has similarities besides convexity to the LDF in the symmetric case. In particular we have from (3.3) that

$$\begin{aligned} \mathcal{F}_{[a,b]}(\{\rho(x)\}; \rho_a, \rho_b) &\geq \int_a^b dx h(\rho(x), \bar{\rho}; \bar{\rho}) \\ &\equiv \mathcal{F}_{[a,b]}^{\text{eq}}(\{\rho(x)\}; \bar{\rho}), \quad \text{if } \rho_a \geq \rho_b, \end{aligned} \quad (3.9)$$

where

$$\mathcal{F}_{[a,b]}^{\text{eq}}(\{\rho(x)\}; \bar{\rho}) = \int_a^b \left[\rho(x) \log \frac{\rho(x)}{\bar{\rho}} + (1 - \rho(x)) \log \frac{1 - \rho(x)}{1 - \bar{\rho}} \right] dx \quad (3.10)$$

is the LDF for an equilibrium system at density $\bar{\rho}$ (see (1.3)). But in the shock region this inequality is reversed:

$$\mathcal{F}_{[a,b]}(\{\rho(x)\}; \rho_a, \rho_b) \leq \mathcal{F}_{[a,b]}^{\text{eq}}(\{\rho(x)\}; \bar{\rho}), \quad \text{if } \rho_a \leq \rho_b, \quad (3.11)$$

as can be derived from (3.1) and (3.4), since in region B_1 (A_1), taking $y = a$ ($y = b$) on the right side of (3.4) gives $\mathcal{F}_{[a,b]}^{\text{eq}}(\{\rho(x)\}; \bar{\rho})$. On the line S , where $\bar{\rho} = \rho_y(x)$ (see (2.1)) for some y , (3.11) holds for all values of y . Physically, (3.9) and (3.11) mean that the probability of a macroscopic deviation from the typical density profile is reduced in the fan region, and increased in the shock region, compared with the probability of the same deviation in an equilibrium system with the same typical profile.

3.5. Flat Density Profiles

One can readily compute the LDF for constant profiles $\rho(x) = r$. In the fan region $\rho_a > \rho_b$ one finds, as discussed in Section 3.1, that F_ρ is also constant, with $F_\rho = \rho_a$ if $r < 1 - \rho_a$, $F_\rho = 1 - r$ if $1 - \rho_a \leq r \leq 1 - \rho_b$, and $F_\rho = \rho_b$ if $1 - \rho_b < r$. There are correspondingly three different expressions for the LDF $\hat{\mathcal{F}}(r) \equiv \mathcal{F}_{[a,b]}(r; \rho_a, \rho_b)$:

$$\hat{\mathcal{F}}(r) = \begin{cases} (b-a) h(r, \rho_a; \bar{\rho}), & \text{if } r < 1 - \rho_a, \\ (b-a) h(r, 1-r; \bar{\rho}), & \text{if } 1 - \rho_a \leq r \leq 1 - \rho_b, \\ (b-a) h(r, \rho_b; \bar{\rho}), & \text{if } 1 - \rho_b < r. \end{cases} \quad (3.12)$$

If $\rho_a > 1/2 > \rho_b$, so that $\bar{\rho} = 1/2$, (phase C of Fig. 1) and $1 - \rho_a \leq r \leq 1 - \rho_b$, then from (3.12),

$$\hat{\mathcal{F}}(r) = 2\mathcal{F}_{[a,b]}(r; 1/2, 1/2) = 2\mathcal{F}_{[a,b]}^{\text{eq}}(r; 1/2), \quad (3.13)$$

where again (see (3.10)) $\mathcal{F}_{[a,b]}^{\text{eq}}(r; 1/2)$ is the large deviation function for observing the uniform density r in a Bernoulli measure with density $1/2$. In particular, for $\rho_a = 1, \rho_b = 0$, the probability of observing all sites empty, $r = 0$, or all sites occupied, $r = 1$, is 2^{-N} for the Bernoulli measure, where $N = L(b-a)$ is the number of sites, so that from (3.13) the corresponding probability for the ASEP is given to leading order by 4^{-N} .

In the shock region $\rho_a < \rho_b$, the minimizing y in (1.11) is $y = b$ if $r < r^*$ and $y = a$ if $r > r^*$, where

$$r^* = \frac{\log \frac{\rho_b}{\rho_a}}{\log \left(\frac{1 - \rho_a \rho_b}{1 - \rho_b \rho_a} \right)} \quad (3.14)$$

so that

$$\hat{\mathcal{F}}(r) = \begin{cases} (b-a) h(r, \rho_a; \bar{\rho}), & \text{if } r \leq r^*, \\ (b-a) h(r, \rho_b; \bar{\rho}), & \text{if } r \geq r^*. \end{cases} \quad (3.15)$$

At $r = r^*$ the derivative is discontinuous, with

$$\left. \frac{d\hat{\mathcal{F}}}{dr} \right|_{r \rightarrow r^*-0} > \left. \frac{d\hat{\mathcal{F}}}{dr} \right|_{r \rightarrow r^*+0}. \quad (3.16)$$

Thus $\hat{\mathcal{F}}(r)$ is not convex near $r = r^*$, and hence $\mathcal{F}_{[a,b]}(\{\rho(x)\}; \rho_a, \rho_b)$ is not convex in a neighborhood of $\rho(x) = r^*$.

3.6. Distribution of the Total Number of Particles

The probability $P_L(M)$ that there are a total of $M = rN$ particles in the system can be obtained from the LDF as

$$-\frac{1}{L} \log P_L(rN) \simeq \tilde{\mathcal{F}}(r) \equiv \mathcal{F}_{[a,b]}(\{\rho(x)\}; \rho_a, \rho_b), \quad (3.17)$$

where $\rho(x)$ is the most likely profile under the constraint

$$\int_a^b \rho(x) dx = r(b-a). \quad (3.18)$$

It will be shown in Appendix B that $\rho(x)$ is the constant profile $\rho(x) = r$, and correspondingly $\tilde{\mathcal{F}}(r) = \hat{\mathcal{F}}(r)$, except in that portion of the shock region in which r satisfies $1 - \rho_b < r < 1 - \rho_a$, where

$$\rho(x) = \begin{cases} 1 - \rho_b, & \text{if } x < y_r, \\ 1 - \rho_a, & \text{if } x > y_r, \end{cases} \quad (3.19)$$

with

$$y_r = \frac{b(1 - \rho_a - r) - a(1 - \rho_b - r)}{\rho_b - \rho_a}. \quad (3.20)$$

Then from (3.4) it follows that for these values of r ,

$$\tilde{\mathcal{F}}(r) = (b-a)[r \log(1 - \rho_a)(1 - \rho_b) + (1-r) \log \rho_a \rho_b - K(\rho_a, \rho_b)]. \quad (3.21)$$

Remarks. (a) Equation (3.19) is easy to interpret on the first order line S in the phase plane, where $\rho_a + \rho_b = 1$: it corresponds there to a typical shock configuration $\rho_{y_r}(x)$, with y_r determined by (3.18).

(b) Although, as observed in Section 3.5, $\hat{\mathcal{F}}$ is not convex (at least in the shock region), $\tilde{\mathcal{F}}$ is always convex, and is in fact the convex envelope of $\hat{\mathcal{F}}$.

(c) We will discuss in Section 6.3 how (3.21) may be derived by a direct calculation from the matrix method.

3.7. Small Fluctuations

It is natural to ask about the connection between the LDF, which gives the probabilities of macroscopic deviations from the typical density profile, and the distribution of small fluctuations, i.e., those of order

$1/\sqrt{N}$. (In what follows we will refer to these simply as “fluctuations.”) In the symmetric case discussed in ref. 15, as in an equilibrium system not at a phase transition (in any dimension, with N being the number of sites in the system), the distribution of fluctuations can be obtained from \mathcal{F} as a limit. More precisely if we write $\rho(x) = \bar{\rho}(x) + \frac{1}{\sqrt{L}} u(x)$ and then expand \mathcal{F} to second order (the first order term being zero) we get a Gaussian distribution for $u(x)$ with covariance $C(x, x')$, where $C^{-1}(x, x') = \delta^2 \mathcal{F} / \delta \rho(x) \delta \rho(x')$ evaluated at $\rho = \bar{\rho}$. This covariance is the suitably scaled microscopic truncated pair correlation.⁽¹⁵⁾

For the asymmetric case discussed in this paper, however, the distribution of small fluctuations need no longer be given by the LDF, as we discuss in Section 6.1. In fact we show there that $\delta^2 \mathcal{F} / \delta \rho(x) \delta \rho(x')$ is discontinuous at $\bar{\rho} = 1/2$ in the interior of region C of the phase diagram, i.e., where $\rho_a > 1/2 > \rho_b$. Furthermore, the fluctuations in this region are no longer Gaussian; in Section 6.3 we show this by computing explicitly the non-Gaussian distribution of the fluctuations of the number of particles in a box of size Ly , with $0 < y < 1$.

4. THE MATRIX METHOD FOR THE ASEP

The steady state properties of the ASEP with open boundaries can be calculated exactly in various ways;^(21, 27, 28) here we describe the so-called matrix method,^(12, 17–19) which we will use in the derivation of the additivity relations in Section 5. Let us consider two operators denoted by D and E , a left vector $\langle W |$ and a right vector $|V\rangle$, which satisfy the following algebraic rules:

$$DE - qED = D + E, \quad (4.1)$$

$$\beta D |V\rangle = |V\rangle, \quad (4.2)$$

$$\langle W | \alpha E = \langle W |. \quad (4.3)$$

Any matrix element of the form $\langle W | Y_1 Y_2 \cdots Y_k |V\rangle / \langle W |V\rangle$, where Y_i denotes D or E , can be calculated from these rules (without the need of writing down an explicit representation). Thus from (4.2, 4.3), one has $\langle W | D |V\rangle / \langle W |V\rangle = 1/\beta$ and $\langle W | E |V\rangle / \langle W |V\rangle = 1/\alpha$, and the matrix element of any product of n matrices can be expressed through (4.1)–(4.3) in terms of sums of elements of shorter products.

For the open ASEP as described in Section 1, the probability $P(\{\tau_i\})$ of the microscopic configuration $\{\tau_i\}$ in the steady state can be written as⁽¹²⁾

$$P(\{\tau_i\}) = \frac{\langle W | \prod_{i=1}^N (D\tau_i + E(1 - \tau_i)) |V\rangle}{Z_N}, \quad (4.4)$$

where $\tau_i = 1$ or 0 indicates whether site i is occupied or empty and the normalization factor Z_N is given by

$$Z_N = \langle W | (D + E)^N | V \rangle. \tag{4.5}$$

On the dashed line $\rho_a = \rho_b$ of Fig. 1, there exists a one dimensional representation of the matrix algebra; it then follows immediately from (4.4) that the invariant measure is Bernoulli on this line. There are other lines in the ρ_a, ρ_b plane where there exist finite dimensional representations^(29, 30) of the algebra (4.1)–(4.3), but the large deviation function has no particular or remarkable expression along these lines, and so these cases will be treated together with the general case.

From the algebra (4.1)–(4.3) all (equal time) steady state properties can (in principle) be calculated. For example the average occupation $\langle \tau_i \rangle$ of site i is given by

$$\langle \tau_i \rangle = \frac{\langle W | (D + E)^{i-1} D (D + E)^{N-i} | V \rangle}{Z_N}, \tag{4.6}$$

and the two point function is, for $i < j$,

$$\langle \tau_i \tau_j \rangle = \frac{\langle W | (D + E)^{i-1} D (D + E)^{j-i-1} D (D + E)^{N-j} | V \rangle}{Z_N}. \tag{4.7}$$

The average steady state current J_N is the same across any bond. It has the form

$$\begin{aligned} J_N &= \langle \tau_i (1 - \tau_{i+1}) - q (1 - \tau_i) \tau_{i+1} \rangle \\ &= \frac{\langle W | (D + E)^{i-1} (DE - qED) (D + E)^{N-i-1} | V \rangle}{Z_N} = \frac{Z_{N-1}}{Z_N}. \end{aligned} \tag{4.8}$$

The probability $\mathcal{Q}_{N_1, \dots, N_k}(M_1, \dots, M_k)$ that there are exactly M_1 particles on the first N_1 sites, M_2 particles on the next N_2 sites, ..., M_k particles in the rightmost N_k sites is given by

$$\mathcal{Q}_{N_1, \dots, N_k}(M_1, \dots, M_k) = \frac{\langle W | Y_1 \cdots Y_k | V \rangle}{Z_N}, \tag{4.9}$$

with

$$Y_p = \frac{1}{2i\pi} \int_0^{2\pi} d\theta e^{-i\theta M_p} (D e^{i\theta} + E)^{N_p}. \tag{4.10}$$

Clearly by making the number k of boxes, and their sizes N_p , large enough, we can approximate any density profile $\rho(x)$ via $\rho(x) = M_p/N_p$ for $x = N^{-1} \sum_{j=1}^p N_j$. Equation (4.9) then gives the probability of the profile $\rho(x)$, and one may attempt to obtain an asymptotic form via a saddle point analysis. This approach, which is conceptually straightforward and was followed in the symmetric case,⁽¹⁵⁾ turns out to be more difficult to implement in the asymmetric case, and this is why we here follow the additivity approach explained in Section 5.

Various more explicit expressions may be extracted from (4.6) and (4.7); for example, in the totally asymmetric case ($q = 0$) the average profile $\langle \tau_i \rangle$ near the boundaries was computed for all i in ref. 12. Moreover, for $q = 0$ and at the special point $\alpha = \beta = 1$ ($\rho_a = 1$ and $\rho_b = 0$) in the maximal current phase C , finite-size corrections have been computed⁽²⁸⁾ for the mean density profile $\langle \tau_i \rangle$ and for the two point function $\langle \tau_i \tau_j \rangle - \langle \tau_i \rangle \langle \tau_j \rangle$. In particular it was found in ref. 28 that at a point $i = Nx$ (with $1 \leq i \leq N$) of a system of N sites,

$$\langle \tau_i \rangle = \frac{1}{2} + \frac{1}{2\sqrt{\pi}} \frac{1}{N^{1/2}} \frac{1-2x}{\sqrt{x(1-x)}} + O(N^{-3/2}), \quad (4.11)$$

which for a system of $N = L(b-a)$ sites becomes for $i = L(x-a)$

$$\langle \tau_i \rangle = \frac{1}{2} + \frac{1}{2\sqrt{\pi}} \frac{1}{L^{1/2}} \frac{b+a-2x}{\sqrt{(b-a)(b-x)(x-a)}} + O(L^{-3/2}). \quad (4.12)$$

Also, at this point ($\alpha = \beta = 1$) of the phase diagram it was shown⁽²⁸⁾ that for large N , the variance of the total number M of particles is given by

$$\langle M^2 \rangle - \langle M \rangle^2 \simeq \frac{N}{8}, \quad (4.13)$$

while a Bernoulli distribution at density $1/2$ would give twice this variance (see the discussion in Section 3.5).

5. DERIVATION OF THE ADDITIVITY FORMULAE

In this section we obtain the additivity formulae (1.6) and (1.10) for the large deviation functional in the ASEP. We begin by deriving two formulae valid for arbitrary system size N . The first of these, (5.10), is obtained directly from the matrix formalism of Section 4 and is valid for a range of parameters corresponding to the fan region $\rho_a > \rho_b$. By analytic continuation of (5.10) we then obtain a new formula (5.24), which is valid

for all parameter values. Finally, we analyze the large N behavior of (5.24) to obtain (1.6) and (1.10).

For $q = 0$, the additivity formula (5.10) takes a much simpler form, which is given in ref. 31. We do not reproduce this formula in the current paper because the treatment here of the general case $0 \leq q < 1$ requires slightly different notations.

5.1. Preliminaries

Let D and E satisfy (4.1)–(4.3) with $q < 1$. We define the operators d and e by

$$D = \frac{1}{1-q} (1+d), \quad E = \frac{1}{1-q} (1+e); \quad (5.1)$$

from (4.1) these operators satisfy

$$de - q ed = 1 - q. \quad (5.2)$$

We also define eigenvectors $|z\rangle$ and $\langle z|$ of d and e , for arbitrary complex z , by

$$d |z\rangle = z |z\rangle, \quad (5.3)$$

$$\langle z| e = \frac{1}{z} \langle z|. \quad (5.4)$$

If X is a polynomial in the operators D and E (or equivalently d and e), then the matrix element $\langle z_0 | X |z_1\rangle / \langle z_0 | z_1\rangle$ is a polynomial in $1/z_0$ and z_1 , with positive coefficients whenever the coefficients in X are positive; this is easily seen since then X is a polynomial in d and e with positive coefficients, and using (5.2) one can push all the d 's to the right and all the e 's to the left, maintaining this positivity.

Finally, we define the function $\varphi(z)$ by

$$\varphi(z) = \sum_{n=0}^{\infty} \frac{1}{c_n} z^n, \quad (5.5)$$

where the c_n are constructed from the recursion

$$c_0 = 1, \quad c_n = (1 - q^n) c_{n-1}. \quad (5.6)$$

One can check easily from (5.5) that

$$\varphi(z) - \varphi(qz) = z\varphi(z), \tag{5.7}$$

so that

$$\varphi(z) = \prod_{n=0}^{\infty} \frac{1}{1 - q^n z}. \tag{5.8}$$

5.2. Exact Additivity Formula for $|z_0| > |z_1|$

The additivity formula which we prove in this section is that if X_0 and X_1 are arbitrary polynomials in the operators D and E , then for

$$|z_0| > |z_1| \tag{5.9}$$

one has

$$\begin{aligned} & \frac{\langle z_0 | X_0 X_1 | z_1 \rangle}{\langle z_0 | z_1 \rangle} \varphi\left(\frac{z_1}{z_0}\right) \\ &= \frac{1}{\varphi(q)} \sum_{n=0}^{\infty} \frac{q^n}{c_n} \oint \frac{dz}{2\pi iz} \frac{\langle z_0 | X_0 | q^n z \rangle}{\langle z_0 | q^n z \rangle} \varphi\left(\frac{q^n z}{z_0}\right) \frac{\langle z | X_1 | z_1 \rangle}{\langle z | z_1 \rangle} \varphi\left(\frac{z_1}{z}\right), \end{aligned} \tag{5.10}$$

where the contour of integration is a circle $|z| = R$ with

$$|z_1| < R < |z_0|. \tag{5.11}$$

Proof. Using (5.2), any polynomial X in D and E can be written in the form

$$X = \sum_{p, p'} A_{p, p'} e^{p'} d^p. \tag{5.12}$$

As (5.10) is linear in X_0 and X_1 , it is sufficient to prove it for $X_0 = e^{p'_0} d^{p_0}$ and $X_1 = e^{p'_1} d^{p_1}$, and as $\langle z_0 |$ and $|z_1 \rangle$ are eigenvectors of e and d , one can immediately simplify the problem and limit the discussion to the case

$$X_0 = d^{p_0}, \quad X_1 = e^{p_1}. \tag{5.13}$$

For this choice of X_0 and X_1 , the right hand side of (5.10) becomes

$$\frac{1}{\varphi(q)} \sum_{n=0}^{\infty} \sum_{m_0=0}^{\infty} \sum_{m_1=0}^{\infty} \frac{q^{n(1+m_0+p_0)}}{c_n c_{m_0} c_{m_1}} \frac{z_1^{m_1}}{z_0^{m_0}} \delta_{m_0+p_0, m_1+p_1}, \tag{5.14}$$

once $\varphi(q^n z/z_0)$ and $\varphi(z_1/z)$ have been replaced by their power series (5.5) and the integration over z has been carried out. One can now use (5.5) again to evaluate the sum over n , and then simplify the result using the identity $\varphi(q^{1+m}) = c_m \varphi(q)$, which follows from (5.7) by an inductive argument, to see that with the choice (5.13),

$$\begin{aligned} \text{r.h.s. of (5.10)} &= \sum_{m_0=0}^{\infty} \sum_{m_1=0}^{\infty} \frac{\varphi(q^{1+m_0+p_0})}{\varphi(q)} \frac{1}{c_{m_0} c_{m_1}} \frac{z_1^{m_1}}{z_0^{m_0}} \delta_{m_0+p_0, m_1+p_1} \\ &= \sum_{m_0=0}^{\infty} \sum_{m_1=0}^{\infty} \frac{c_{m_0+p_0}}{c_{m_0} c_{m_1}} \frac{z_1^{m_1}}{z_0^{m_0}} \delta_{m_0+p_0, m_1+p_1}. \end{aligned} \tag{5.15}$$

So to prove (5.10), we just need to show that the left hand side of (5.10), again with the choice (5.13), coincides with (5.15).

We argue by induction on p_0 . If $p_0 = 0$, it is easy to see that the left hand side of (5.10) is given by $z_0^{-p_1} \varphi(z_1/z_0)$. Evaluating (5.15) in this case leads to the same expression.

Let us assume, then, that (5.10) is valid for all $p_0 \leq P$. We want to prove that it remains true for $p_0 = P + 1$. To do so we observe the following consequence of (5.2):

$$d^{P+1} e^{p_1} = (1 - q^{p_1}) d^P e^{p_1-1} + q^{p_1} d^P e^{p_1} d. \tag{5.16}$$

Using (5.16), the left hand side of (5.10) for $p_0 = P + 1$, i.e., for $X_0 = d^{P+1}$ and $X_1 = e^{p_1}$, becomes

$$(1 - q^{p_1}) \frac{\langle z_0 | d^P e^{p_1-1} | z_1 \rangle}{\langle z_0 | z_1 \rangle} \varphi\left(\frac{z_1}{z_0}\right) + q^{p_1} \frac{\langle z_0 | d^P e^{p_1} d | z_1 \rangle}{\langle z_0 | z_1 \rangle} \varphi\left(\frac{z_1}{z_0}\right). \tag{5.17}$$

As we have hypothesized that (5.10) is valid for $p_0 \leq P$, we can replace each term of (5.17) by the corresponding expressions (5.15), leading to

$$\begin{aligned} \text{l.h.s. of (5.10)} &= \sum_{m_0=0}^{\infty} \sum_{m_1=0}^{\infty} \frac{c_{m_0+P}}{c_{m_0} c_{m_1}} \frac{z_1^{m_1}}{z_0^{m_0}} \\ &\times [(1 - q^{p_1}) \delta_{m_0+P, m_1+p_1-1} + z_1 q^{p_1} \delta_{m_0+P, m_1+p_1}]. \end{aligned} \tag{5.18}$$

If now in the second term in (5.18) we make the change of summation index $m_1 \rightarrow m_1 - 1$, and then use the identities $c_{m_1} = (1 - q^{m_1}) c_{m_1-1}$ and $c_{m_0+P+1} = (1 - q^{m_0+P+1}) c_{m_1}$, we obtain

$$\text{l.h.s. of (5.10)} = \sum_{m_0=0}^{\infty} \sum_{m_1=0}^{\infty} \frac{c_{m_0+P+1}}{c_{m_0} c_{m_1}} \frac{z_1^{m_1}}{z_0^{m_0}} \delta_{m_0+P+1, m_1+p_1}, \tag{5.19}$$

which is identical for $p_0 = P + 1$ to (5.15). This completes the derivation of (5.10).

5.3. Analytic Continuation of (5.10)

Recall that (5.10) has been established for $|z_0| > |z_1|$, with integration contour a circle $|z| = R$ with $|z_1| < R < |z_0|$. However, the left hand side of this equation is an analytic function defined for all complex z_0 and z_1 except at $z_0 = 0$ and at the poles of $\varphi(z_1/z_0)$. In this section we make an analytic continuation of the right hand side to obtain an integral representation of the left side which is valid for any z_0, z_1 for which the left side is defined. In the final representation we will again integrate over a contour $|z| = R$, but now R will be allowed to take any value for which the contour does not pass through singularities of the integrand, that is, for which

$$R > 0, \quad R \neq q^m |z_1|, \quad m \geq 0, \quad R \neq q^{-m} |z_0|, \quad m \geq 0. \quad (5.20)$$

The expression on the right hand side of (5.10) must be modified when, as one varies z_0, z_1 and R , the singularities of the integrand—that is, the poles of $\varphi(q^n z/z_0)$ and $\varphi(z_1/z)$ —cross the integration contour. When this happens, however, the residue theorem tells us how (5.10) is to be modified: one simply includes the residue of the pole on the right hand side of the equation, adding or subtracting it according to whether the pole crosses the contour from the inside to the outside or vice versa. Using the fact that the residue of $\varphi(z)$ at $z = q^{-m}$, $m = 0, 1, \dots$, is

$$\frac{(-1)^{m+1} q^{m(m-1)/2}}{c_m} \varphi(q), \quad (5.21)$$

one then finds the following extension of (5.10):

Suppose that R satisfies (5.20). If $R < |z_1|$ then define k_1 by

$$q^{k_1+1} |z_1| < R < q^{k_1} |z_1|, \quad (5.22)$$

and if $R > |z_0|$ define k_0 by

$$\frac{|z_0|}{q^{k_0}} < R < \frac{|z_0|}{q^{k_0+1}}. \quad (5.23)$$

Then

$$\begin{aligned}
 & \frac{\langle z_0 | X_0 X_1 | z_1 \rangle}{\langle z_0 | z_1 \rangle} \varphi \left(\frac{z_1}{z_0} \right) \\
 &= \sum_{n=0}^{\infty} \frac{q^n}{c_n} \left\{ \frac{1}{\varphi(q)} \oint_{|z|=R} \frac{dz}{2\pi iz} \frac{\langle z_0 | X_0 | q^n z \rangle}{\langle z_0 | q^n z \rangle} \varphi \left(\frac{q^n z}{z_0} \right) \frac{\langle z | X_1 | z_1 \rangle}{\langle z | z_1 \rangle} \varphi \left(\frac{z_1}{z} \right) \right. \\
 & \quad + \Theta(|z_1| - R) \sum_{m=0}^{k_1} \frac{(-1)^m q^{m(m+1)/2}}{c_m} \varphi \left(\frac{q^{n+m} z_1}{z_0} \right) \\
 & \quad \times \frac{\langle z_0 | X_0 | q^{n+m} z_1 \rangle}{\langle z_0 | q^{n+m} z_1 \rangle} \frac{\langle q^m z_1 | X_1 | z_1 \rangle}{\langle q^m z_1 | z_1 \rangle} \\
 & \quad + \Theta(R - q^{-n} |z_0|) \sum_{m=0}^{k_0-n} \frac{(-1)^m q^{m(m+1)/2}}{c_m} \varphi \left(\frac{q^{n+m} z_1}{z_0} \right) \\
 & \quad \left. \times \frac{\langle z_0 | X_0 | q^{-m} z_0 \rangle}{\langle z_0 | q^{-m} z_0 \rangle} \frac{\langle q^{-(n+m)} z_0 | X_1 | z_1 \rangle}{\langle q^{-(n+m)} z_0 | z_1 \rangle} \right\}. \tag{5.24}
 \end{aligned}$$

5.4. Asymptotics of the Additivity Formula

We now ask what happens to the representation (5.24) when the system size N becomes very large. Throughout this section we take z_0 and z_1 to be positive real numbers and X_0 and X_1 to be polynomials, with positive coefficients, in the operators D and E . We will use throughout this section three properties of the product

$$\Pi_n(z) \equiv \frac{\langle z_0 | X_0 | q^n z \rangle}{\langle z_0 | q^n z \rangle} \frac{\langle z | X_1 | z_1 \rangle}{\langle z | z_1 \rangle} \tag{5.25}$$

occurring in the integrands of the representation (5.24), which follow from the discussion of Section 5.1: $\Pi_n(z)$ is a polynomial in $q^n z$ and $1/z$, with positive coefficients; for z on the positive real axis, $\Pi_n(z)$ is a convex function of z ; for fixed positive z , $\Pi_n(z)$ decreases as n increases. We will assume that, for z on the positive axis, $\Pi_n(z)$ grows exponentially in N .

Now $\Pi_0(z)$ has a unique minimum at some value z_{\min} on the positive real axis; we will use the representation (5.24) with the choice $R = z_{\min}$. Using first the fact that the maximum of the magnitude $|\Pi_n(z)|$ on the contour $|z| = z_{\min}$ occurs on the real axis, and then the monotonicity of $\Pi_n(z)$ in n for z positive, we see that each integral occurring in (5.24) satisfies

$$\begin{aligned}
 & \left| \oint_{|z|=z_{\min}} \frac{dz}{2\pi iz} \frac{\langle z_0 | X_0 | q^n z \rangle}{\langle z_0 | q^n z \rangle} \varphi\left(\frac{q^n z}{z_0}\right) \frac{\langle z | X_1 | z_1 \rangle}{\langle z | z_1 \rangle} \varphi\left(\frac{z_1}{z}\right) \right| \\
 & \lesssim \frac{\langle z_0 | X_0 | q^n z_{\min} \rangle}{\langle z_0 | q^n z_{\min} \rangle} \frac{\langle z_{\min} | X_1 | z_1 \rangle}{\langle z_{\min} | z_1 \rangle}, \\
 & \leq \frac{\langle z_0 | X_0 | z_{\min} \rangle}{\langle z_0 | z_{\min} \rangle} \frac{\langle z_{\min} | X_1 | z_1 \rangle}{\langle z_{\min} | z_1 \rangle}, \tag{5.26}
 \end{aligned}$$

where the first inequality holds up to factors that do not grow exponentially with N . On the other hand, when $n = 0$ the point z_{\min} will be a saddle point for $\Pi_0(z)$ lying on the contour $|z| = z_{\min}$, and equality (again up to factors not growing exponentially with N) will hold in (5.26).

The bound (5.26), and an argument similar to that above for the terms in (5.24) arising from the poles, show that the $n = 0$ terms there always dominate those with $n > 0$, so that we may neglect the latter. But for $n = 0$, the fact that $\Pi_0(z)$ is convex, with a minimum at z_{\min} , implies that the $m = 0$ terms dominate each sum over m . Thus (5.24) becomes (again up to factors not growing exponentially with N)

$$\begin{aligned}
 \frac{\langle z_0 | X_0 X_1 | z_1 \rangle}{\langle z_0 | z_1 \rangle} & \sim \max \left\{ \frac{\langle z_0 | X_0 | z_{\min} \rangle}{\langle z_0 | z_{\min} \rangle} \frac{\langle z_{\min} | X_1 | z_1 \rangle}{\langle z_{\min} | z_1 \rangle}, \right. \\
 & \quad \Theta(z_1 - z_{\min}) \frac{\langle z_0 | X_0 | z_1 \rangle}{\langle z_0 | z_1 \rangle} \frac{\langle z_1 | X_1 | z_1 \rangle}{\langle z_1 | z_1 \rangle}, \\
 & \quad \left. \Theta(z_{\min} - z_0) \frac{\langle z_0 | X_0 | z_0 \rangle}{\langle z_0 | z_0 \rangle} \frac{\langle z_0 | X_1 | z_1 \rangle}{\langle z_0 | z_1 \rangle} \right\}. \tag{5.27}
 \end{aligned}$$

Now the discussion can be completed by considering successively all the possible relative positions of z_0, z_1 and z_{\min} .

Suppose first that $z_1 < z_0$. Then (5.27) gives

$$\frac{\langle z_0 | X_0 X_1 | z_1 \rangle}{\langle z_0 | z_1 \rangle} \simeq \begin{cases} \frac{\langle z_0 | X_0 | z_{\min} \rangle}{\langle z_0 | z_{\min} \rangle} \frac{\langle z_{\min} | X_1 | z_1 \rangle}{\langle z_{\min} | z_1 \rangle}, & \text{if } z_1 < z_{\min} < z_0, \\ \frac{\langle z_0 | X_0 | z_1 \rangle}{\langle z_0 | z_1 \rangle} \frac{\langle z_1 | X_1 | z_1 \rangle}{\langle z_1 | z_1 \rangle}, & \text{if } z_{\min} < z_1 < z_0, \\ \frac{\langle z_0 | X_0 | z_0 \rangle}{\langle z_0 | z_0 \rangle} \frac{\langle z_0 | X_1 | z_1 \rangle}{\langle z_0 | z_1 \rangle}, & \text{if } z_1 < z_0 < z_{\min}, \end{cases} \tag{5.28}$$

and one sees that each case in (5.28) reduces to

$$\frac{\langle z_0 | X_0 X_1 | z_1 \rangle}{\langle z_0 | z_1 \rangle} \simeq \min_{z_1 \leq z \leq z_0} \frac{\langle z_0 | X_0 | z \rangle \langle z | X_1 | z_1 \rangle}{\langle z_0 | z \rangle \langle z | z_1 \rangle}. \tag{5.29}$$

On the other hand, if $z_0 < z_1$, then (5.27) gives

$$\frac{\langle z_0 | X_0 X_1 | z_1 \rangle}{\langle z_0 | z_1 \rangle} \simeq \begin{cases} \max_{z = z_0, z_1} \frac{\langle z_0 | X_0 | z \rangle \langle z | X_1 | z_1 \rangle}{\langle z_0 | z \rangle \langle z | z_1 \rangle}, & \text{if } z_0 < z_{\min} < z_1, \\ \frac{\langle z_0 | X_0 | z_1 \rangle \langle z_1 | X_1 | z_1 \rangle}{\langle z_0 | z_1 \rangle \langle z_1 | z_1 \rangle}, & \text{if } z_{\min} < z_0 < z_1, \\ \frac{\langle z_0 | X_0 | z_0 \rangle \langle z_0 | X_1 | z_1 \rangle}{\langle z_0 | z_0 \rangle \langle z_0 | z_1 \rangle}, & \text{if } z_0 < z_1 < z_{\min}, \end{cases} \tag{5.30}$$

and each case in (5.30) reduces to

$$\frac{\langle z_0 | X_0 X_1 | z_1 \rangle}{\langle z_0 | z_1 \rangle} \simeq \max_{z = z_0, z_1} \frac{\langle z_0 | X_0 | z \rangle \langle z | X_1 | z_1 \rangle}{\langle z_0 | z \rangle \langle z | z_1 \rangle}. \tag{5.31}$$

5.5. Derivation of (1.6) and (1.10)

We finally want to obtain the fundamental additivity relations for \mathcal{H} , (1.6) and (1.10), from (5.29) and (5.31). The first step is to relate the densities ρ_a, ρ_b to the parameters z_0, z_1 . Using (1.1), (5.3), and (5.4), one can easily establish that if

$$\rho_a = \frac{z_0}{1 + z_0}, \quad \rho_b = \frac{z_1}{1 + z_1}, \tag{5.32}$$

then

$$\frac{\langle z_0 | X_0 X_1 | z_1 \rangle}{\langle z_0 | z_1 \rangle} = \frac{\langle W | X_0 X_1 | V \rangle}{\langle W | V \rangle}, \tag{5.33}$$

where $\langle W |$ and $|V \rangle$ are defined by (4.2) and (4.3).

Now let us consider a given profile $\rho(x)$ defined for $a < x < b$, and for fixed c with $a < c < b$ denote by X_0 the sum over all the products of D 's and E 's consistent with the left part of this profile over the first $L(c-a)$

sites, and by X_1 the same quantity for the right part of the profile over the last $L(b-c)$ sites. We define \mathcal{H} by

$$(1-q)^{L(b-a)} \frac{\langle z_0 | X_0 X_1 | z_1 \rangle}{\langle z_0 | z_1 \rangle} \sim \exp[-L\mathcal{H}_{[a,b]}(\{\rho(x)\}; \rho_a, \rho_b)]. \quad (5.34)$$

Then we obtain immediately (1.6) and (1.10) from (5.29) and (5.31). Moreover from (1.2), (4.4), (5.33), and (5.34) we see that the constant $K(\rho_a, \rho_b)$ which appears in (1.4) is given by

$$(1-q)^{L(b-a)} \langle W | (D+E)^{L(b-a)} | V \rangle \sim e^{-L(b-a)K(\rho_a, \rho_b)}. \quad (5.35)$$

Writing (5.29) and (5.31) for $X_0 = (D+E)^{L(c-a)}$ and $X_1 = (D+E)^{L(b-c)}$, we see that $K(\rho_a, \rho_b)$ should satisfy

$$(b-a)K(\rho_a, \rho_b) = \sup_{\rho_b \leq \rho_c \leq \rho_a} [(c-a)K(\rho_a, \rho_c) + (b-c)K(\rho_c, \rho_b)], \quad (5.36)$$

if $\rho_a > \rho_b$, and

$$(b-a)K(\rho_a, \rho_b) = \min_{\rho_c = \rho_a \text{ or } \rho_b} [(c-a)K(\rho_a, \rho_c) + (b-c)K(\rho_c, \rho_b)], \quad (5.37)$$

if $\rho_a < \rho_b$. Now when $\rho_a = \rho_b$ the matrices D and E commute and may be realized as the scalars $D = (1-q)^{-1}(1+z_0)$, $E = (1-q)^{-1}(1+z_0^{-1})$, so that from (5.35) and (5.32) we have

$$K(\rho_a, \rho_a) = -\log\left(z_0 + 2 + \frac{1}{z_0}\right) = \log[\rho_a(1-\rho_a)]. \quad (5.38)$$

From (5.36) and (5.38) one finds, by repeated subdivision of the interval $[a, b]$, that if $\rho_a > \rho_b$ then

$$(b-a)K(\rho_a, \rho_b) = \sup_f \int_a^b dx \log[f(x)(1-f(x))], \quad (5.39)$$

where the supremum is over nonincreasing functions $f(x)$ with $f(a) = \rho_a$ and $f(b) = \rho_b$, and from (5.39) one obtains (1.5). Similarly, if $\rho_a < \rho_b$ one obtains from (5.36) and (5.38) that

$$(b-a)K(\rho_a, \rho_b) = \inf_{a \leq y \leq b} \left\{ \int_a^y dx \log[\rho_a(1-\rho_a)] + \int_y^b dx \log[\rho_b(1-\rho_b)] \right\}, \quad (5.40)$$

and (1.9) follows.

6. LARGE DEVIATIONS VERSUS TYPICAL FLUCTUATIONS

Expressions (1.7) and (1.11) enable us to calculate the large deviation function for an arbitrary density profile $\rho(x)$. As we have already noted and will show in this section, the large deviation functional, which describes macroscopic (order N) deviations from the typical profile $\bar{\rho}$, is in region C , where

$$\rho_a > \frac{1}{2} > \rho_b, \tag{6.1}$$

not simply related to the fluctuations (order \sqrt{N}) around $\bar{\rho}$. We demonstrate this by computing explicitly, for $q=0$, the probability of seeing a given global density r in a window $c < x < d$ of our system, with no other constraint in the system, both for fixed r with $r \neq \bar{\rho}$ and for $r - \bar{\rho}$ of order $1/\sqrt{N}$.

We divide our system of $N = L(b-a)$ sites into three boxes, of $N_1 = L(c-a)$ sites, $N_2 = L(d-c)$ sites and $N_3 = N(b-d)$ sites, corresponding to macroscopic intervals $[a, c]$, $[c, d]$, and $[d, b]$, and compute the probability that the density is r in the middle box, i.e., the probability $P(M_2)$ that the total number M_2 of particles in the middle box is

$$M_2 = L(d-c)r, \tag{6.2}$$

with no constraint imposed in the two other boxes.

6.1. Large Deviation

Corresponding to the above constraint there will be an optimal profile $\rho(x)$ for which, with $\bar{\mathcal{F}}(r) \equiv \bar{\mathcal{F}}_{[a,b]}(\rho(x); \rho_a, \rho_b)$, one has

$$P(M_2) \sim \exp[-L\bar{\mathcal{F}}]. \tag{6.3}$$

Since $\rho_a > \rho_b$, one can use the additivity formula (1.6)

$$\begin{aligned} \mathcal{H}_{[a,b]}(\rho(x); \rho_a, \rho_b) = & \sup_{\rho_b \leq \rho_d \leq \rho_c \leq \rho_a} \{ \mathcal{H}_{[a,c]}(\rho(x); \rho_a, \rho_c) \\ & + \mathcal{H}_{[c,d]}(\rho(x); \rho_c, \rho_d) + \mathcal{H}_{[d,b]}(\rho(x); \rho_d, \rho_b) \}. \end{aligned} \tag{6.4}$$

As there is no constraint on the profile in the two side boxes, one has $\mathcal{F}_{[a,c]}(\rho(x); \rho_a, \rho_c) = \mathcal{F}_{[d,b]}(\rho(x); \rho_d, \rho_b) = 0$, so that from (1.4),

$$\mathcal{H}_{[a,c]}(\rho(x); \rho_a, \rho_c) = (c-a) K(\rho_a, \rho_c), \tag{6.5}$$

$$\mathcal{H}_{[b,d]}(\rho(x); \rho_d, \rho_b) = (b-d) K(\rho_d, \rho_b). \tag{6.6}$$

Moreover, since $\rho_c \geq \rho_d$ we know from Sections 3.5 and 3.6 that within the central box $[c, d]$ the optimal profile $\rho(x)$, which corresponds to a fixed number of particles there, is flat. From (1.4) and (3.12) we then have

$$\mathcal{H}_{[c,d]}(\rho(x); \rho_c, \rho_d) = \begin{cases} (c-d)[r \log(r(1-\rho_c)) + (1-r) \log((1-r)\rho_c)], \\ (c-d)[2r \log r + 2(1-r) \log(1-r)], \\ (c-d)[r \log(r(1-\rho_d)) + (1-r) \log((1-r)\rho_d)], \end{cases} \quad (6.7)$$

when $r < 1 - \rho_c$, $1 - \rho_c < r < 1 - \rho_d$, and $1 - \rho_d < r$, respectively. Now from (6.4) one must choose ρ_c and ρ_d to maximize the sum of (6.5), (6.6), and (6.7). The result depends on the sign of $r - 1/2$.

Case 1. $r < 1/2$. In this case the optimizing values of ρ_c and ρ_d are

$$\rho_c = \min \left\{ \frac{(d-a) - r(d-c)}{d+c-2a}, \rho_a \right\}, \quad \rho_d = \frac{1}{2}. \quad (6.8)$$

The corresponding LDF is

$$\begin{aligned} \bar{\mathcal{F}}(r) &= (d-c)[r \log(4r(1-\rho_c)) + (1-r) \log(4(1-r)\rho_c)] \\ &\quad + (c-a) \log(4\rho_c(1-\rho_c)), \end{aligned} \quad (6.9)$$

which for r close to $1/2$ becomes

$$\bar{\mathcal{F}}(r) = \frac{4(d-c)(d-a)}{d+c-2a} \left(r - \frac{1}{2} \right)^2 + O \left(r - \frac{1}{2} \right)^3. \quad (6.10)$$

We also find from Section 3.2 that the optimal profile $\rho(x)$ satisfies $\rho(x) = \rho_c$ for $a < x < c$ and $\rho(x) = 1/2$ for $d < x < b$.

Case 2. $r > 1/2$. In this case, a similar calculation leads to

$$\rho_c = \frac{1}{2}, \quad \rho_d = \max \left\{ \frac{(b-c) - r(d-c)}{2b-d-c}, \rho_b \right\} \quad (6.11)$$

and

$$\begin{aligned} \bar{\mathcal{F}}(r) &= (d-c)[r \log(4r(1-\rho_d)) + (1-r) \log(4(1-r)\rho_d)] \\ &\quad + (b-d) \log(4\rho_d(1-\rho_d)); \end{aligned} \quad (6.12)$$

and for r close to $1/2$, (6.12) gives

$$\bar{\mathcal{F}} = \frac{4(d-c)(b-c)}{2b-c-d} \left(r - \frac{1}{2}\right)^2 + O\left(r - \frac{1}{2}\right)^3. \tag{6.13}$$

We see from (6.10) and (6.13) that in general the limiting value of the second derivative of $\bar{\mathcal{F}}(r)$ at $r = 1/2$ depends on the sign of $r - 1/2$, so that $\bar{\mathcal{F}}(r)$ is in general nonanalytic at $r = 1/2$. Note, however, that when the overall density for the system is specified, i.e., when $c = a$ and $d = b$, $\bar{\mathcal{F}}(r)$ is analytic.

6.2. Fluctuations

Formulae (6.9) and (6.12), with (6.8) and (6.11), give us the leading behavior of $P(M_2)$ for large deviations, i.e., for $r - 1/2$ of order 1. Let us now discuss the small fluctuations, i.e., the regime in which $r - 1/2 = O(L^{-1/2})$, so that $L\bar{\mathcal{F}}$ is of order one. As (6.10) and (6.13) do not coincide, one expects that typical fluctuations around the optimal profile $\bar{\rho}(x) = 1/2$ will be anomalous, i.e., non-Gaussian. Let us define the fluctuation μ in the number M_2 of particles in the central box by

$$M_2 - \frac{(d-c)L}{2} = \mu \sqrt{L}. \tag{6.14}$$

In the next subsection we will derive, for $q = 0$, the following probability density $p(\mu) = P(M_2) \sqrt{L}$ for the random variable μ :

$$\begin{aligned} p(\mu) &= \frac{8(b-a)^{3/2}}{[\pi(c-a)(b-d)]^{3/2} (d-c)} \\ &\times \int_0^\infty dx \int_0^\infty dy xy \exp\left[-\frac{x^2}{c-a} - \frac{y^2}{b-d}\right] \\ &\times \left\{ \exp\left[-2\frac{\mu^2 + (\mu+x-y)^2}{d-c}\right] - \exp\left[-2\frac{(\mu+x)^2 + (\mu-y)^2}{d-c}\right] \right\}. \end{aligned} \tag{6.15}$$

We see that indeed μ has a non-Gaussian distribution. Note, however, that the \sqrt{L} scaling in (6.14) is that appropriate for “normal” fluctuations.

For large positive μ , (6.15) becomes

$$p(\mu) = \frac{4}{\mu\pi} \frac{(b-a)^{3/2} (b-c)(b-d)}{(d-c)^{1/2} (2b-c-d)^{3/2} (c-a)^{3/2}} \exp\left[-\frac{4(b-c)}{(d-c)(2b-d-c)} \mu^2\right], \tag{6.16}$$

and for large negative μ ,

$$p(\mu) = \frac{4}{|\mu| \pi} \frac{(b-a)^{3/2} (d-a)(c-a)}{(d-c)^{1/2} (d+c-2a)^{3/2} (b-d)^{3/2}} \exp \left[-\frac{4(d-a)}{(d-c)(d+c-2a)} \mu^2 \right]. \tag{6.17}$$

We see that the large μ asymptotics (6.16) and (6.17) match with (6.10) and (6.13) when $|\mu| \gg 1$ and $|r-1/2| \ll 1$, with $\mu = (r-1/2)(d-c) \sqrt{L}$, i.e., that (6.15) interpolates between the large deviation regions $r > 1/2$ and $r < 1/2$.

Also, from (6.15) one can compute the average $\langle \mu \rangle$ of μ :

$$\langle \mu \rangle = \int p(\mu) \mu d\mu = \frac{\sqrt{(d-a)(b-d)} - \sqrt{(c-a)(b-c)}}{\sqrt{\pi} \sqrt{b-a}}. \tag{6.18}$$

For a system of $N = L(b-a)$ sites, one sees from (4.12) that

$$\sum_{i=L(c-a)}^{L(d-a)} \left(\langle \tau_i \rangle - \frac{1}{2} \right) = \frac{\sqrt{L}}{2\sqrt{\pi}} \int_c^d \frac{b+a-2x}{\sqrt{(b-a)(b-x)(x-a)}} dx, \tag{6.19}$$

in agreement with (6.18), since $\langle M_2 \rangle - L(d-c)/2 = \langle \mu \rangle \sqrt{L}$.

6.3. Derivation of (6.15)

One way to derive (6.15) is to use the following explicit representation⁽¹²⁾ of (4.1), valid for $q = 0$:

$$D = \sum_{n=1}^{\infty} |n\rangle \langle n| + |n\rangle \langle n+1|, \tag{6.20}$$

$$E = \sum_{n=1}^{\infty} |n\rangle \langle n| + |n+1\rangle \langle n|, \tag{6.21}$$

where the vectors $|1\rangle, |2\rangle, \dots, |n\rangle, \dots$ form an orthonormal basis of an infinite dimensional space (with $\langle n | m \rangle = \delta_{n,m}$). Within this basis, the vectors $|V\rangle$ and $\langle W|$ are given (see (4.2), (4.3), and (1.1)) by

$$|V\rangle = \sum_{n=1}^{\infty} \left(\frac{1-\beta}{\beta} \right)^n |n\rangle = \sum_{n=1}^{\infty} \left(\frac{\rho_b}{1-\rho_b} \right)^n |n\rangle, \tag{6.22}$$

$$\langle W| = \sum_{n=1}^{\infty} \left(\frac{1-\alpha}{\alpha} \right)^n \langle n| = \sum_{n=1}^{\infty} \left(\frac{1-\rho_a}{\rho_a} \right)^n \langle n|, \tag{6.23}$$

and one can show (for example by recursion) that

$$\langle p | (D + E)^N | p' \rangle = \frac{(2N)!}{(N + p - p')! (N + p' - p)!} - \frac{(2N)!}{(N + p + p')! (N - p' - p)!} \quad (6.24)$$

and that^(32, 33)

$$\begin{aligned} \langle p | X_{N, M} | p' \rangle &= \frac{(N!)^2}{(M)! (N - M)! (M + p - p')! (N - M - p + p')!} \\ &\quad - \frac{(N!)^2}{(M + p)! (N - M - p)! (M - p')! (N - M + p')!} \end{aligned} \quad (6.25)$$

where $X_{N, M}$ is the sum over all the configurations of N sites with M occupied particles. The probability $P(M_2)$ that the number of particles is M_2 in the central box is given by

$$P(M_2) = \frac{\langle W | (D + E)^{N_1} X_{N_2, M_2} (D + E)^{N_3} | V \rangle}{\langle W | (D + E)^{N_1 + N_2 + N_3} | V \rangle}. \quad (6.26)$$

From (6.26) one may recover the results of Section 3.4.

Let us first analyze the denominator of (6.26):

$$\langle W | (D + E)^N | V \rangle = \sum_{p_1=1}^{\infty} \sum_{p_2=1}^{\infty} \left(\frac{1 - \rho_a}{\rho_a} \right)^{p_1} \left(\frac{\rho_b}{1 - \rho_b} \right)^{p_2} \langle p_1 | (D + E)^N | p_2 \rangle. \quad (6.27)$$

For large N , this sum is dominated by p_1 and p_2 of order 1, so one can use an approximation of (6.24) valid for p and p' of order \sqrt{N} or less,

$$\langle p | (D + E)^N | p' \rangle \simeq \frac{4^N}{\sqrt{\pi N}} \left[\exp \left(\frac{-(p - p')^2}{N} \right) - \exp \left(\frac{-(p + p')^2}{N} \right) \right], \quad (6.28)$$

and one gets for large N ,

$$\langle W | (D + E)^N | V \rangle \simeq \frac{4^{N+1}}{\sqrt{\pi} N^{3/2}} \frac{(1 - \rho_a) \rho_a (1 - \rho_b) \rho_b}{(2\rho_a - 1)^2 (2\rho_b - 1)^2}. \quad (6.29)$$

One can write the numerator of (6.26) as

$$\begin{aligned} \langle W | (D + E)^{N_1} X_{N_2, M_2} (D + E)^{N_3} | V \rangle &= \sum_{p_1} \sum_{p_2} \sum_{p_3} \sum_{p_4} \langle W | p_1 \rangle \\ &\langle p_1 | (D + E)^{N_1} | p_2 \rangle \langle p_2 | X_{N_2, M_2} | p_3 \rangle \langle p_3 | (D + E)^{N_3} | p_4 \rangle \langle p_4 | V \rangle. \end{aligned} \quad (6.30)$$

When N_1, N_2, N_3 are large and of order L and when the difference $M_2 - N_2/2$ is of order \sqrt{L} as in (6.14), these sums are dominated by p_1 and p_4 of order 1 and p_2 and p_3 of order \sqrt{L} . If one writes

$$p_2 = x \sqrt{L}, \quad p_3 = y \sqrt{L}, \quad (6.31)$$

one gets that

$$\begin{aligned} \langle p_2 | X_{N_2, M_2} | p_3 \rangle &\simeq 4^{N_2} \frac{2}{\pi N_2} \left[\exp \left(-\frac{2L}{N_2} (\mu^2 + (\mu + x - y)^2) \right) \right. \\ &\left. - \exp \left(-\frac{2L}{N_2} ((\mu - y)^2 + (\mu + x)^2) \right) \right], \end{aligned} \quad (6.32)$$

and the numerator becomes, after summing over p_1 and p_4 and replacing the sums over p_2 and p_3 by integrals,

$$\begin{aligned} &\langle W | (D + E)^{N_1} X_{N_2, M_2} (D + E)^{N_3} | V \rangle \\ &= \frac{4^{N_1 + N_2 + N_3 + 2} \times 2}{\pi^2 L^2 [(c - a)(b - d)]^{3/2} (d - c)} \\ &\times \frac{(1 - \rho_a) \rho_a}{(2\rho_a - 1)^2} \frac{(1 - \rho_b) \rho_b}{(2\rho_b - 1)^2} \int_0^\infty dx \int_0^\infty dy xy \exp \left[-\frac{x^2}{c - a} - \frac{y^2}{b - d} \right] \\ &\times \left\{ \exp \left[-2 \frac{\mu^2 + (\mu + x - y)^2}{d - c} \right] - \exp \left[-2 \frac{(\mu + x)^2 + (\mu - y)^2}{d - c} \right] \right\} \end{aligned} \quad (6.33)$$

which reduces to (6.15) after dividing by (6.29).

Remark. One can also recover from (6.26) the expressions (6.9) and (6.12) by allowing deviations in M_2 of order L .

7. CONCLUSION

The main results of the present work are the exact expressions (1.7) and (1.11) for the LDF $\mathcal{F}(\{\rho\})$ for the SNS of the open ASEP in one

dimension and the simple additivity formulae (1.6) and (1.10) that they satisfy.

This \mathcal{F} , like the one we found for the symmetric case in refs. 15 and 16, is a non-local functional of the density profile $\{\rho(x)\}$. We expect non-locality to be a general feature of such functionals for non-equilibrium systems.

Our expressions of the LDF, which take different forms in the fan region $\rho_a > \rho_b$ (where the reservoirs and the bulk asymmetry cooperate) and in the shock region $\rho_a < \rho_b$ (where they act in opposite directions), reflect several qualitative differences:

In the fan region, $\rho_a > \rho_b$, the probability of macroscopic deviations from the typical density profile is reduced compared with that in an equilibrium system with the same typical profile (see (3.9)); this was also true in the symmetric case.⁽¹⁶⁾ Another surprising feature of the fan region, at least in the maximal current phase C, is that the fluctuations of the density profile cannot be calculated from the LDF, and that these fluctuations are in general not Gaussian (see Section 6). We have no heuristic explanation of this behavior.

In the shock region of the phase diagram, $\rho_a < \rho_b$, \mathcal{F} is not convex in ρ (see Section 3.3). Moreover, in this region the probability of macroscopic deviations from typical behavior is increased rather than reduced; see (3.11). This enhancement of deviations appears similar to known behavior⁽⁸⁾ of fluctuations (the behavior of macroscopic deviations is not known) in a slab of fluid in contact at the top with a heat reservoir at temperature T_a , and at the bottom with another reservoir at temperature T_b : the Rayleigh–Bénard system.⁽⁶⁾ In this system the force of gravity causes the SNS to undergo dynamic phase transitions when $(T_b - T_a)$ is “sufficiently” large, corresponding to different spatial patterns of heat and mass flow. This transition is preceded, as $T_b - T_a$ is increased, by enhanced fluctuations even for very small differences between the two temperatures (for which the system is stable) as long as $T_b > T_a$.

It is natural to expect that the probabilities of typical fluctuations and of large deviations are either both enhanced or both reduced, in comparison with the equilibrium ρ system having the same $\bar{\rho}$, but this is not known to be true in general. In fact, our work here shows that small (typical) fluctuations cannot in general be computed from the LDF.

One can note that our expressions for the LDF (1.7) and (1.11) do not depend on the asymmetry parameter $0 \leq q < 1$. These expressions, however, are not valid at $q = 1$, and they do not reproduce the symmetric exclusion result: the limits $q \rightarrow 1$ and $N \rightarrow \infty$ do not commute. It would be interesting to analyze the case of large N with $1 - q = O(N^{-1})$, in order to interpolate between the symmetric case and the asymmetric case.

It would also be desirable to have a physical understanding of our additivity formulae (1.6) and (1.10), and to see how our results could be generalized to more complicated non-equilibrium steady states.

Lastly, from our knowledge of the LDF in the SNS steady state, one could try to determine how a given (unlikely) profile was produced dynamically out of the nonequilibrium steady state. This has been done for the symmetric exclusion process on a circle in ref. 34, and recently for the open system in refs. 35 and 36, where the LDF was given in terms of a time integral over a trajectory taking the system, via a “reversed dynamics,” from a typical SNS configuration to the profile $\rho(x)$. A dynamic LDF for the ASEP on the circle was studied in ref. 37.

APPENDIX A. THE CONCAVE ENVELOPE CONSTRUCTION

In this appendix we justify the construction (3.5, 3.6) of the optimizing function F_ρ for the supremum in (1.7). Recall that we are given a density profile $\rho(x)$ which is defined for $a \leq x \leq b$ and satisfies $0 \leq \rho(x) \leq 1$ for all x , and reservoir densities ρ_a and ρ_b which satisfy $1 \geq \rho_a > \rho_b \geq 0$. Let $H_\rho(x) = \int_a^x (1 - \rho(y)) dy$, so that G_ρ is the concave envelope of H_ρ , and recall that F_ρ is obtained by cutting off $G'_\rho(x)$ at ρ_a and ρ_b (see (3.6)). Then (1.7) may be written as

$$\begin{aligned} & \mathcal{F}_{[a,b]}(\{\rho(x)\}; \rho_a, \rho_b) \\ &= -(b-a) K(\rho_a, \rho_b) + \int_a^b dx [\rho(x) \log \rho(x) + (1 - \rho(x)) \log(1 - \rho(x))] \\ & \quad + \sup_{F(x)} B_\rho(F), \end{aligned} \tag{A.1}$$

where

$$B_\rho(F) = \int_a^b dx \left[(1 - \rho(x)) \log \frac{F(x)}{1 - F(x)} + \log(1 - F(x)) \right], \tag{A.2}$$

and the supremum in (A.1) is over monotone nonincreasing functions $F(x)$ satisfying $F(a) = \rho_a$, $F(b) = \rho_b$. Now since $H_\rho(x) \leq G_\rho(x)$ for all x and $\log[F(x)/1 - F(x)]$ is decreasing, we obtain by integration by parts, noting that $H(a) = G(a)$ and $H(b) = G(b)$, that for any $F(x)$ in this class,

$$\begin{aligned} & \int_a^b dx [(1 - \rho(x)) - G'_\rho(x)] \log \frac{F(x)}{1 - F(x)} \\ &= - \int_a^b [H_\rho(x) - G_\rho(x)] d \left[\log \frac{F(x)}{1 - F(x)} \right] \leq 0, \end{aligned} \tag{A.3}$$

so that

$$B_\rho(F) \leq \int_a^b dx \left[G'_\rho(x) \log \frac{F(x)}{1-F(x)} + \log(1-F(x)) \right]. \tag{A.4}$$

Since the integrand in (A.4) is pointwise concave in $F(x)$, with a maximum at $F(x) = G'_\rho(x)$, the integral is, for the functions $F(x)$ satisfying $\rho_a \geq F(x) \geq \rho_b$, bounded above by its value at $F(x) = F_\rho(x)$. Thus

$$\begin{aligned} B_\rho(F) &\leq \int_a^b dx \left[G'_\rho(x) \log \frac{F_\rho(x)}{1-F_\rho(x)} + \log(1-F_\rho(x)) \right] \\ &= \int_a^b dx \left[(1-\rho(x)) \log \frac{F_\rho(x)}{1-F_\rho(x)} + \log(1-F_\rho(x)) \right] \\ &= B_\rho(F_\rho); \end{aligned} \tag{A.5}$$

here the first equality is obtained by noting that if (c, d) is a maximal interval on which $G'_\rho(x) \neq H'_\rho(x)$ then (i) $G'_\rho(x)$ and hence $F_\rho(x)$ are constant on this interval and (ii) $\int_c^d G'_\rho(x) dx = \int_c^d (1-\rho(x)) dx$. Equation (A.5) shows that the supremum in (A.1) is achieved by $F(x) = F_\rho(x)$.

APPENDIX B. OPTIMAL PROFILE UNDER A CONSTRAINT

Let $\rho(x)$ be an optimal system profile for a fixed mean density r , that is, a profile which minimizes $\mathcal{F}_{[a,b]}(\{\rho(x)\}; \rho_a, \rho_b)$ under the constraint

$$\int_a^b \rho(x) dx = r(b-a). \tag{B.1}$$

In this section we show that $\rho(x)$ is uniquely determined, and derive its form.

Case 1. $\rho_a > \rho_b$. Let G_ρ and F_ρ be defined by (3.5) and (3.6), so that

$$\mathcal{F}_{[a,b]}(\{\rho(x)\}; \rho_a, \rho_b) = \int_a^b h(\rho(x), F_\rho(x); \bar{\rho}) dx, \tag{B.2}$$

where $h(r, f; \bar{\rho})$ is defined in (3.2) and $\bar{\rho}$ is determined from ρ_a, ρ_b as in Fig. 1.

We first show that $\rho(x)$ must be monotone nondecreasing, that is, that $\rho(x) = 1 - G'_\rho(x)$ (almost everywhere). For otherwise there will exist some interval $[c, d] \subset [a, b]$ satisfying

$$G_\rho(c) = \int_a^c (1 - \rho(y)) dy, \quad G_\rho(d) = \int_a^d (1 - \rho(y)) dy, \quad (\text{B.3})$$

and

$$G_\rho(x) > \int_a^x (1 - \rho(y)) dy, \quad \text{for } c \leq x \leq d. \quad (\text{B.4})$$

Then for $c \leq x \leq d$, $G'_\rho(x) = 1 - \lambda$, where

$$\lambda = \frac{1}{c-d} \int_c^d \rho(y) dy, \quad (\text{B.5})$$

and if ρ^* is defined by

$$\rho^*(x) = \begin{cases} \lambda, & \text{if } c < x < d, \\ \rho(x), & \text{otherwise,} \end{cases} \quad (\text{B.6})$$

then ρ^* satisfies (B.1) and from the strict convexity of $h(\rho, F; \bar{\rho})$ in ρ and the fact that F_ρ is constant on $[c, d]$ (with value λ , ρ_a , or ρ_b) it follows that

$$(c-d) h(\lambda, F_\rho; \bar{\rho}) < \int_c^d h(\rho(x), F_\rho(x); \bar{\rho}) dx \quad (\text{B.7})$$

and hence that $\mathcal{F}_{[a,b]}(\{\rho^*(x)\}; \rho_a, \rho_b) < \mathcal{F}_{[a,b]}(\{\rho(x)\}; \rho_a, \rho_b)$, contradicting the definition of $\rho(x)$.

Since $\rho(x) = 1 - G'_\rho(x)$ we have from (3.6) that $F_\rho(x)$ is a local function of $\rho(x)$ taking value ρ_a if $1 - \rho(x) > \rho_a$, ρ_b if $1 - \rho(x) < \rho_b$, and $1 - \rho(x)$ otherwise. Then one can check that the integrand $h(\rho(x), F_\rho(x); \bar{\rho})$ in (B.2) is pointwise convex in $\rho(x)$. Thus since $\rho(x)$ satisfies (B.1), $(b-a) h(r, 1-r, \bar{\rho}) \leq \mathcal{F}_{[a,b]}(\{\rho(x)\}; \rho_a, \rho_b)$, with equality if and only if $\rho(x)$ is the constant function $\rho(x) = r$.

Case 2. $\rho_a < \rho_b$. Let y_r be the minimizing value in (1.11) corresponding to the optimal profile $\rho(x)$; it is clear that $\rho(x)$ must be constant on the intervals $[a, y_r]$ and $[y_r, b]$, so that

$$\begin{aligned} & \mathcal{F}_{[a,b]}(\{\rho(x)\}; \rho_a, \rho_b) \\ &= (y_r - a) h(r_a, \rho_a; \bar{\rho}) + (b - y_r) h(r_b, \rho_b; \bar{\rho}) \end{aligned} \quad (\text{B.8})$$

for some values r_a, r_b satisfying

$$(y_r - a) r_a + (b - y_r) r_b = (b - a) r. \quad (\text{B.9})$$

Minimizing (B.8) over $a \leq y_r \leq b$ and (B.9) leads to $y_r = b$, $r_a = r$ if $r < 1 - \rho_b$ and $y_r = a$, $r_b = r$ if $r > 1 - \rho_a$, while if $1 - \rho_b \leq r \leq 1 - \rho_a$, y_r is given by (3.20) and $r_a = 1 - \rho_b$, $r_b = 1 - \rho_a$.

ACKNOWLEDGMENTS

We thank T. Bodineau, G. Giacomin, and J. M. Ortiz de Zárate for helpful discussions. The work of J. L. Lebowitz was supported by NSF Grant DMR-9813268, AFOSR Grant F49620/0154, DIMACS and its supporting agencies, and NATO Grant PST.CLG.976552. J.L.L. acknowledges the hospitality of the Institut Henri Poincaré, and B.D. and J.L.L. that of the Institute for Advanced Study, where a part of this work was done.

REFERENCES

1. S. R. De Groot and P. Mazur, *Non-Equilibrium Thermodynamics* (North-Holland, Amsterdam, 1962).
2. H. Spohn, *Large Scale Dynamics of Interacting Particles* (Springer-Verlag, Berlin, 1991).
3. R. Graham, Onset of cooperative behavior in nonequilibrium steady states, in *Order and Fluctuations in Equilibrium and Nonequilibrium Statistical Mechanics*, G. Nicolis, G. Dewel, and J. W. Turner, eds. (Wiley, New York, 1981).
4. H. Spohn, Long range correlations for stochastic lattice gases in a non-equilibrium steady state, *J. Phys. A.* **16**:4275–4291 (1983).
5. R. Schmitz, Fluctuations in nonequilibrium fluids, *Phys. Reports* **171**:1–58 (1988), and references therein.
6. M. C. Cross and P. C. Hohenberg, Pattern formation outside of equilibrium, *Rev. Mod. Phys.* **65**:851–1112 (1993).
7. J. R. Dorfman, T. R. Kirkpatrick, and J. V. Sengers, Generic long-range correlations in molecular fluids, *Annu. Rev. Phys. Chem.* **45**:213–239 (1994).
8. W. B. Li, K. J. Zhang, J. V. Sengers, R. W. Gammon, and J. M. Ortiz de Zárate, Concentration fluctuations in a polymer solution under a temperature gradient, *Phys. Rev. Lett.* **81**:5580–5583 (1998).
9. S. Sasa and H. Tasaki, cond-mat/0108365 and references therein.
10. T. M. Liggett, *Interacting Particle Systems* (Springer-Verlag, New York, 1985).
11. B. Schmittman and R. K. P. Zia, *Statistical Mechanics of Driven Diffusive Systems* (Academic Press, London, 1995).
12. B. Derrida, M. R. Evans, V. Hakim, and V. Pasquier, Exact solution of a 1D asymmetric exclusion model using a matrix formulation, *J. Phys. A* **26**:1493–1517 (1993).
13. S. Olla, Large deviations for Gibbs random fields, *Probab. Th. Rel. Fields* **77**:343–357 (1988).
14. R. Ellis, *Entropy, Large Deviations, and Statistical Mechanics* (Springer, New York, 1985).

15. B. Derrida, J. L. Lebowitz, and E. R. Speer, Large deviation of the density profile in the symmetric simple exclusion process, *J. Stat. Phys.* **107**:599–634 (2002).
16. B. Derrida, J. L. Lebowitz, and E. R. Speer, Free energy functional for nonequilibrium systems: an exactly solvable case, *Phys. Rev. Lett.* **87**:150601 (2001).
17. S. Sandow, Partial asymmetric exclusion process with open boundaries, *Phys. Rev. E* **50**:2660–2667 (1994).
18. T. Sasamoto, One dimensional partially asymmetric simple exclusion process with open boundaries: Orthogonal polynomials approach, *J. Phys. A* **32**:7109–7131 (1999).
19. R. A. Blythe, M. R. Evans, F. Colaiori, and F. H. L. Essler, Exact solution of a partially asymmetric exclusion model using a deformed oscillator algebra, *J. Phys. A* **33**:2313–2332 (2000).
20. J. Krug, Boundary-induced phase transitions in driven diffusive systems, *Phys. Rev. Lett.* **67**:1882–1885 (1991).
21. G. Schütz and E. Domany, Phase transitions in an exactly soluble one-dimensional exclusion process, *J. Stat. Phys.* **72**:277–296 (1993).
22. T. M. Liggett, *Stochastic Interacting Systems: Contact, Voter, and Exclusion Processes* (Springer-Verlag, New York, 1999).
23. L. Santen and C. Appert, The asymmetric exclusion process revisited: fluctuations and dynamics in the domain wall picture, *J. Stat. Phys.* **106**:187–199 (2002).
24. M. Bramson, Front propagation in certain one-dimensional exclusion models, *J. Stat. Phys.* **51**:863–869 (1988).
25. V. Popkov and G. M. Schütz, Steady state selection in driven diffusive systems with open boundaries, *Europhys. Lett.* **48**:257–263 (1999).
26. J. S. Hager, J. Krug, V. Popkov, and G. M. Schütz, Minimal current phase and universal boundary layers in driven diffusive systems, *Phys. Rev. E* **63**:056100 1–12 (2001).
27. B. Derrida, E. Domany, and D. Mukamel, An exact solution of a one dimensional asymmetric exclusion model with open boundaries, *J. Stat. Phys.* **69**:667–687 (1992).
28. B. Derrida and M. R. Evans, Exact correlation functions in an asymmetric exclusion model with open boundaries, *J. Phys. I France* **3**:311–322 (1993).
29. F. H. L. Essler and V. Rittenberg, Representations of the quadratic algebra and partially asymmetric diffusion with open boundaries, *J. Phys. A* **29**:3375–3408 (1996).
30. K. Mallick and S. Sandow, Finite dimensional representations of the quadratic algebra: applications to the exclusion process, *J. Phys. A* **30**:4513–4526 (1997).
31. B. Derrida, J. L. Lebowitz, and E. R. Speer, Exact free energy functional for a driven diffusive open stationary nonequilibrium system, *Phys. Rev. Lett.* **89**:030601 (2002).
32. B. Derrida, M. R. Evans, and D. Mukamel, Exact diffusion constant for one-dimensional asymmetric exclusion models, *J. Phys. A* **26**:4911–4918 (1993).
33. K. Mallick, Shocks in the asymmetric exclusion model with an impurity, *J. Phys. A* **29**:5375–5386 (1996).
34. C. Kipnis, S. Olla, and S. R. S. Varadhan, Hydrodynamics and large deviations for simple exclusion processes, *Commun. Pure Appl. Math.* **42**:115–137 (1989).
35. L. Bertini, A. De Sole, D. Gabrielli, G. Jona-Lasinio, and C. Landim, Fluctuations in stationary non equilibrium states of irreversible processes, *Phys. Rev. Lett.* **87**:040601 (2001).
36. L. Bertini, A. De Sole, D. Gabrielli, G. Jona-Lasinio, and C. Landim, Macroscopic fluctuation theory for stationary non equilibrium states, *J. Stat. Phys.* **107**:635–675 (2002).
37. L. Jensen, Large deviations of the asymmetric simple exclusion process in one dimension, Dissertation (New York University, 2000).